

Supplementary Information for

**A Multi-site Passive Approach for Studying the
Emissions and Evolution of Smoke from Prescribed
Fires**

Rime El Asmar¹, Zongrun Li², David J. Tanner¹, Yongtao Hu², Susan O'Neill³, L. Gregory Huey¹,
M. Talat Odman², Rodney J. Weber¹

¹Earth and Atmospheric Sciences, Georgia Institute of Technology, Atlanta, 30331, USA.

²School of Civil and Environmental Engineering, Georgia Institute of Technology, Atlanta, 30331, USA.

³USDA Forest Service, Pacific Northwest Research Station, 400 North 34th Street, Suite 201, Seattle, WA 98103,
USA.

Correspondence to: Rodney J. Weber (rweber@eas.gatech.edu)

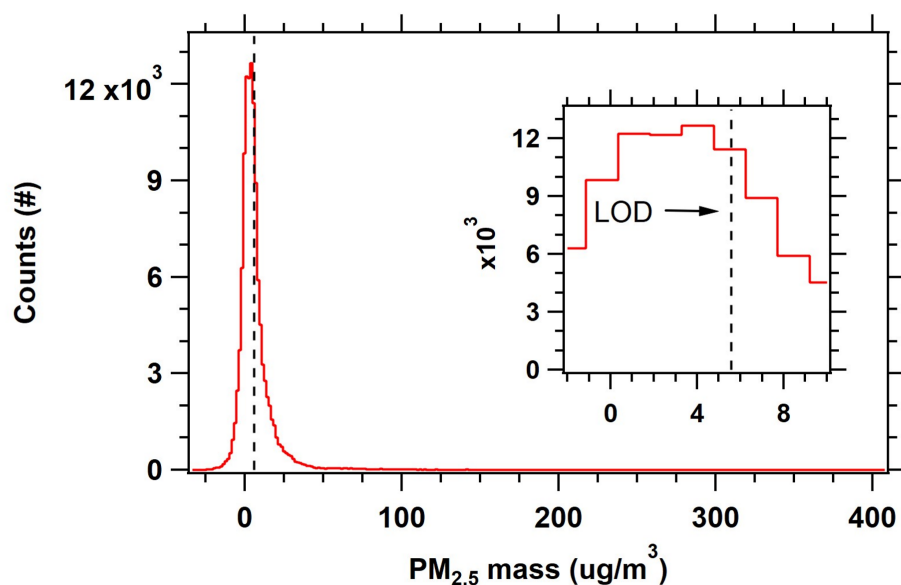
13 S.1 Example on determining the physical age of smoke average wind vector

14 The first identified smoke event in this work took place on March 23, 2021, and is shown in Figure S7.

15 Measured PM_{2.5} mass, CO, and BC start increasing at 12:30 pm and reached a maximum at 3:00 pm.

16 Based on observed wind direction and HYSPLIT back trajectories, the source of the smoke was
17 determined as the prescribed fire that took place on the same day on unit N34 on Fort Moore. The
18 distance from the indicated unit is 8.104 miles at an azimuth of 130° from the measuring site. The average
19 wind vector during the hour leading to the peak is 4 mph at 132°. This means that it takes more than 1
20 hour for smoke to be transported across 8.104 miles. Iteration by averaging the wind vector for the two
21 hours leading to the peak, results in wind vector of speed 4.5 mph at 131.5°. By dividing the distance by
22 the speed calculated, the age estimated is 108 minutes. Since the calculated age is less than 2 hours, no
23 more iteration is needed.

24



26

27 **Figure S1.** Example frequency distribution of PM_{2.5} mass measurements by a TEOM that was installed on
 28 the main trailer during the 2022 field study at Fort Moore. The data was recorded at a rate of every 60 s.
 29 The vertical black dotted line is the estimated LOD base based on three times the standard deviation of
 30 blank measurement. The frequency distribution is conducted with 300 bins and a bin width interval of
 31 1.48 ug m⁻³. The results illustrate the presence of negative measured masses when averaging over short
 32 time intervals.

33

34

35



37

38 **Figure S2.** WRF domain settings. North American Mesoscale Forecast System (NAM) 12km (National
 39 Centers for Environmental Prediction, National Weather Service, NOAA, 2015) data are used to provide
 40 initial and boundary conditions for WRF. WRF simulated the meteorological conditions by the one-way
 41 nesting method for 12km (D01), 4km (D02), and 1km (D03) domains. Global surface and upper air
 42 observational weather data (National Centers for Environmental Prediction, National Weather Service,
 43 NOAA, 2004a, b) are used for grid nudging in all three domains and for observational nudging in the 1km
 44 domain. HYSPLIT used 1km domain outputs from WRF.

45

46

47

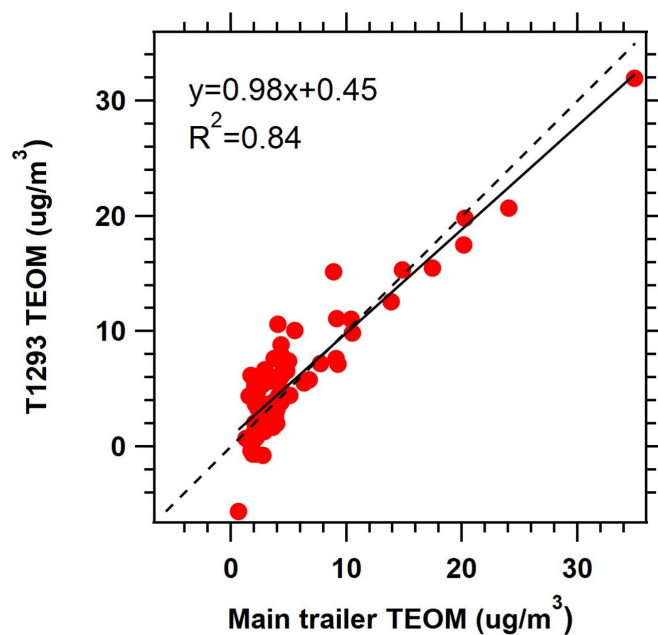
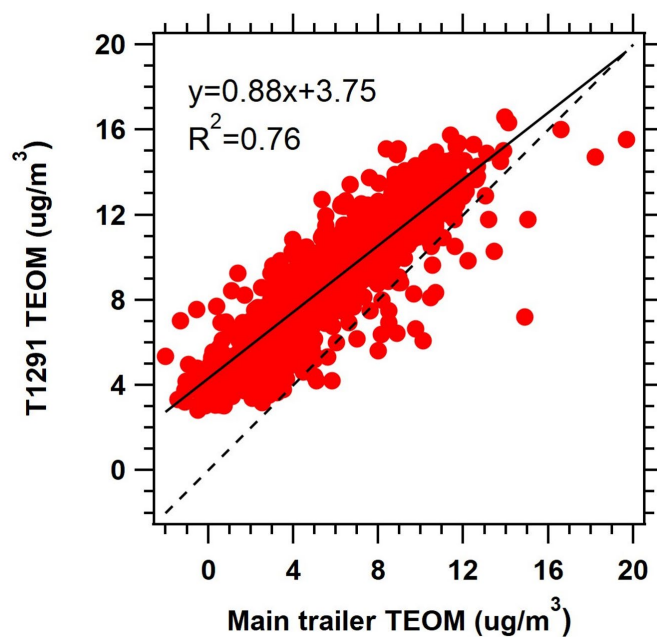


Figure S3. Comparison of PM_{2.5} mass concentrations measured by collocated TEOMs (main trailer TEOM and TEOM in trailer T1293) over a period of 26 hours. The sampling site was Eglin Air Force Base from March 19, 2023 at 8:00 till March 20, 2023 at 10:00. Slope is from orthogonal distance regression (ODR) of the 20-minutes averaged data.

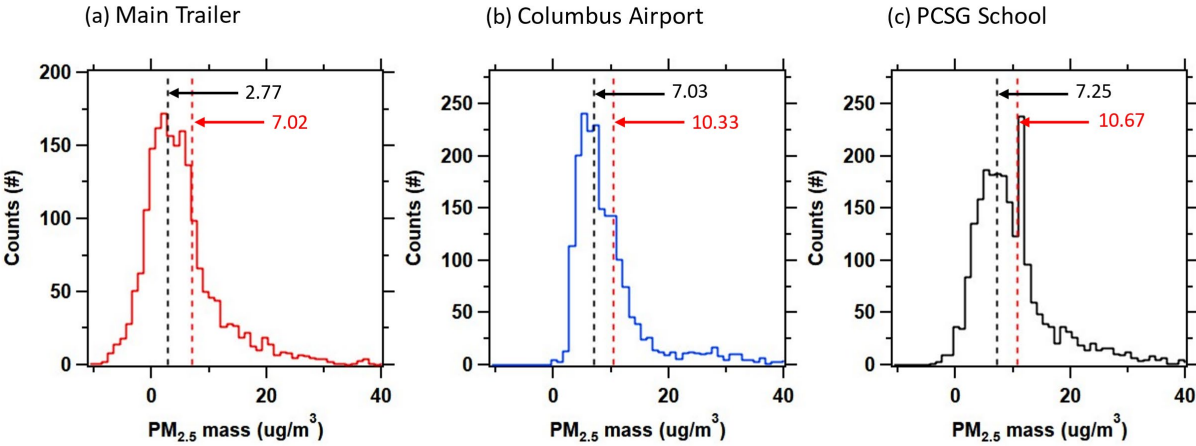
56
57



58
59 **Figure S4.** Comparison of PM_{2.5} mass concentrations measured by collocated TEOMs (main trailer
60 TEOM and TEOM in trailer T1291) over a period of 336 hours. The sampling site was Georgia Institute
61 of Technology, Ford Environmental Science and Technology building from September 22, 2023 at 19:00
62 till October 7, 2023 at 14:00. Slope is from orthogonal distance regression (ODR) of the 20-minutes
63 averaged data.

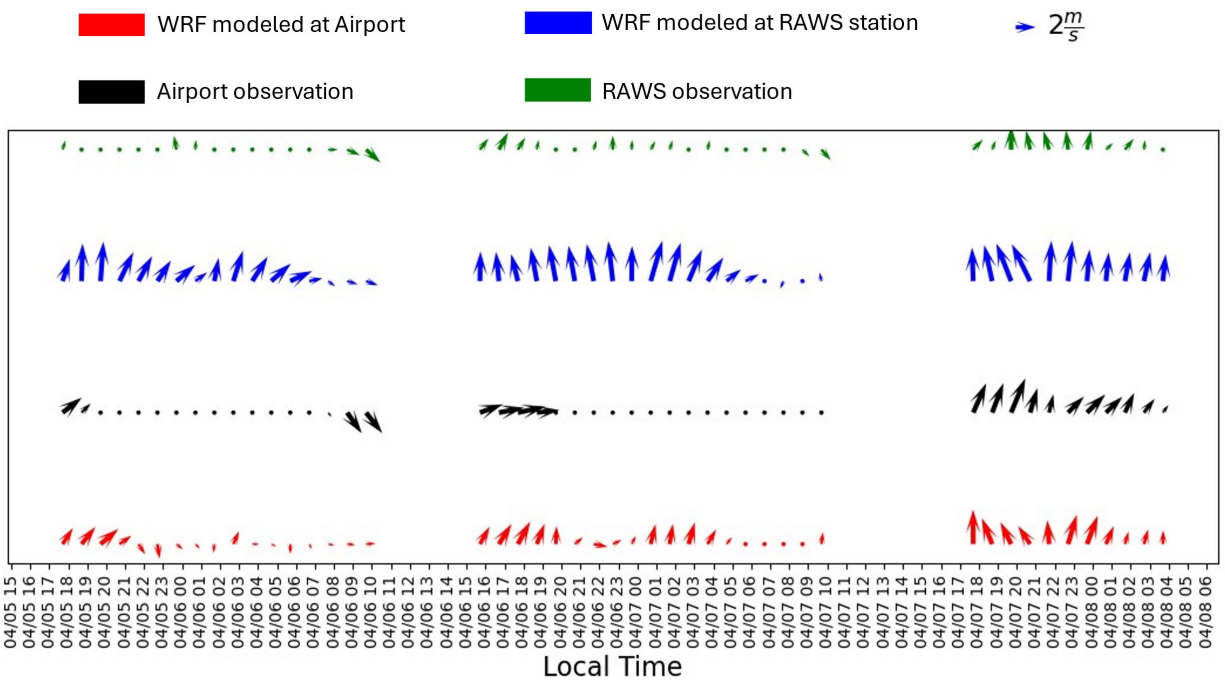
64
65
66

67
68



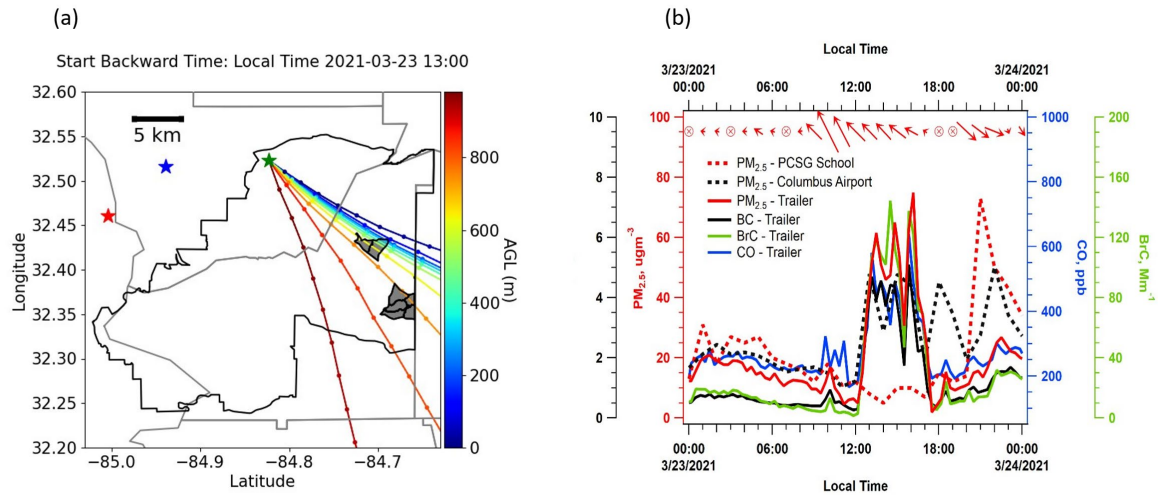
69
70
71
72
73
74
75
76
77
78

Figure S5. Frequency distribution of PM_{2.5} mass measurements taken by the TEOM that was installed in the main trailer and at the two EPD sites (Columbus airport and PCSG school) in field study of 2022 (February 11, 2022 till May 18, 2022). The data are 60-minutes averages. The vertical black dotted line is the calculated mean background PM_{2.5} at each site. The red vertical dotted line is the mean of all data in the frequency distribution of each site. The frequency distribution is conducted with 300 bins and a bin width interval of 1.03 ug m⁻³.



80

81 Figure S6. Wind vectors during the three smoke events shown in Figure 5 representing hourly data
 82 sourced from (i) RAWS station located at Fort Moore, (ii) weather station located at Columbus airport,
 83 (iii) WRF modeled winds at RAWS location, and (iv) WRF modeled winds at the location of weather
 84 station at the airport. The direction of the arrow indicates wind direction, and the length of the arrow
 85 represents wind speed.



87

Figure S7. A case study of two prescribed fires reported on the base but not detected on the satellite. (a) HYSPLIT back trajectories starting on March 23, 2021 at 13:00. The colors of the trajectories represent the height above ground level. Green star marks the location of the main trailer; blue and red stars mark Columbus airport and PCSG school EPD sites respectively. Time and height at which the lowest trajectory crosses the trailer are shown in the box inside the map. The fires detected on FIRMS would have been shown by red dots but there are no detections. Grey shaded Polygons are the boundaries of prescribed burns conducted on the Fort based on the fire reports. (b) Time series of species measured on main trailer. Time resolution is 20 minutes for CO, PM_{2.5} mass, BC, and BrC. Data from PCSG School and Columbus Airport are hourly averages. The wind vectors depict hourly data sourced from RAWS, with the direction of the arrow indicating wind direction, and the length of the arrow representing wind speed.

89

90

91

92

93

94

95

96

97

98

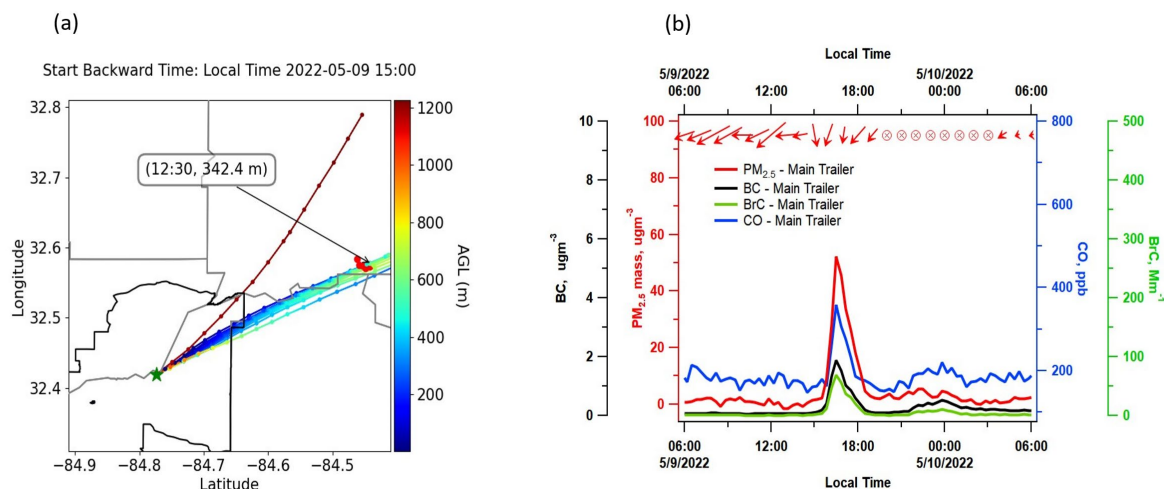


Figure S8. A case study on the influence of off-base fires on smoke detection within the base. (a) HYSPLIT back trajectories starting on May 9, 2022 at 15:00. The colors of the scatter are the height above ground level. Green star marks the location of the main trailer. Time and height at which the lowest trajectory crosses the trailer are shown in the box inside the map. Red dots are fires detected on FIRMS the same day of the backward trajectory (satellite overpass happened on May 9, 2022, at 12:38, 13:54, and 14:42). (b) Time series of species measured on main trailer. Time resolution is 20 minutes for CO, PM_{2.5} mass, BC, and BrC. The wind vectors depict hourly data sourced from RAWS, with the direction of the arrow indicating wind direction, and the length of the arrow representing wind speed.

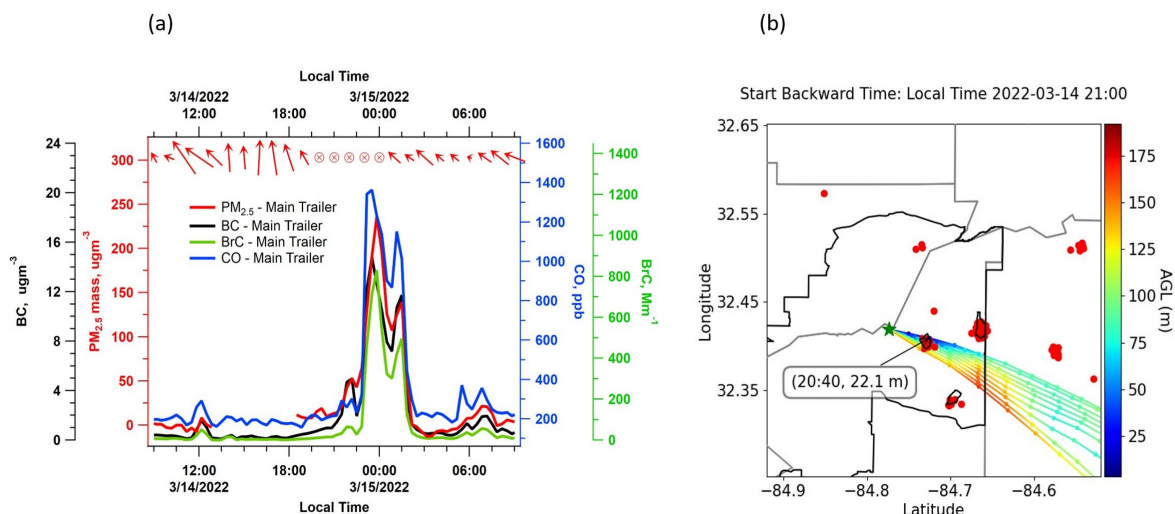
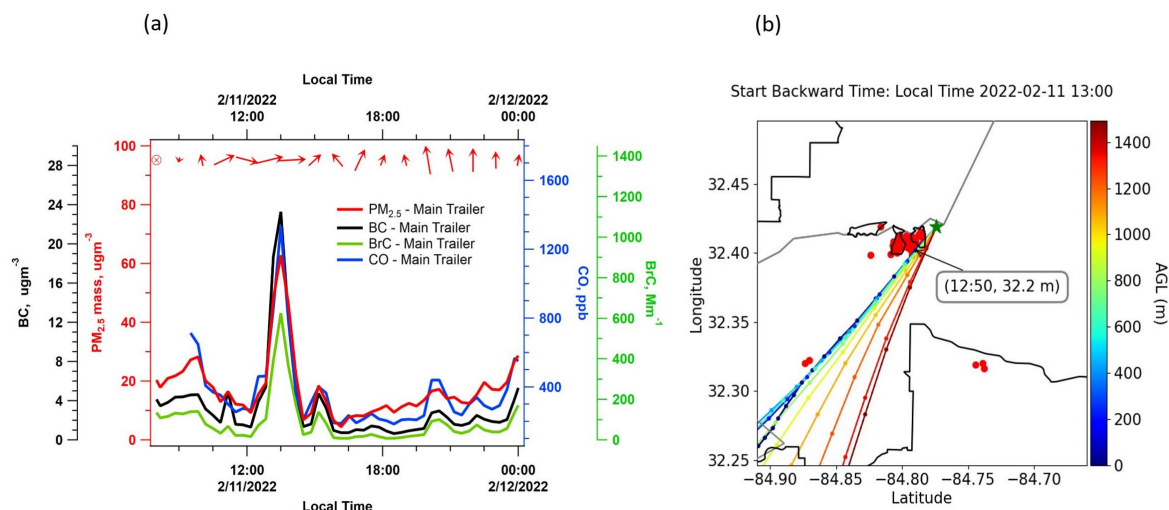


Figure S9. A case study on multiple burns on the same day. (a) Time series of species measured at the main trailer. Time resolution is 20 minutes for CO, PM_{2.5} mass, BC, and BrC. The wind vectors depict hourly data sourced from RAWS, with the direction of the arrow indicating wind direction and the length of the arrow representing wind speed. (b) HYSPLIT back trajectories starting on March 14, 2022, at 21:00. The colors of the scatter are the height above ground level. Green star marks the location of the main trailer. Time and height at which the lowest trajectory crosses the trailer are shown in the box inside the map. Red dots are fires detected on FIRMS the same day of the backward trajectory (satellite overpass happened on March 14, 2022, at 11:51, 13:48, 14:43, and 15:12).



133

Figure S10. A case study of multiple close burns on the same day. (a) Time series of species measured at the main trailer. Time resolution is 20 minutes for CO, $PM_{2.5}$ mass, BC, and BrC. The wind vectors depict hourly data sourced from RAWS, with the direction of the arrow indicating wind direction and the length of the arrow representing wind speed. (b) HYSPLIT back trajectories starting on February 11, 2022 at 13:00. The colors of the scatter are the height above ground level. Green star marks the location of the main trailer. Time and height at which the lowest trajectory crosses the trailer are shown in the box inside the map. Red dots are fires detected on FIRMS the same day of the backward trajectory (satellite overpass happened on February 11, 2022 at 13:19, 13:23, and 14:12).

134

135

136

137

138

139

140

141

142

143

144

145

146

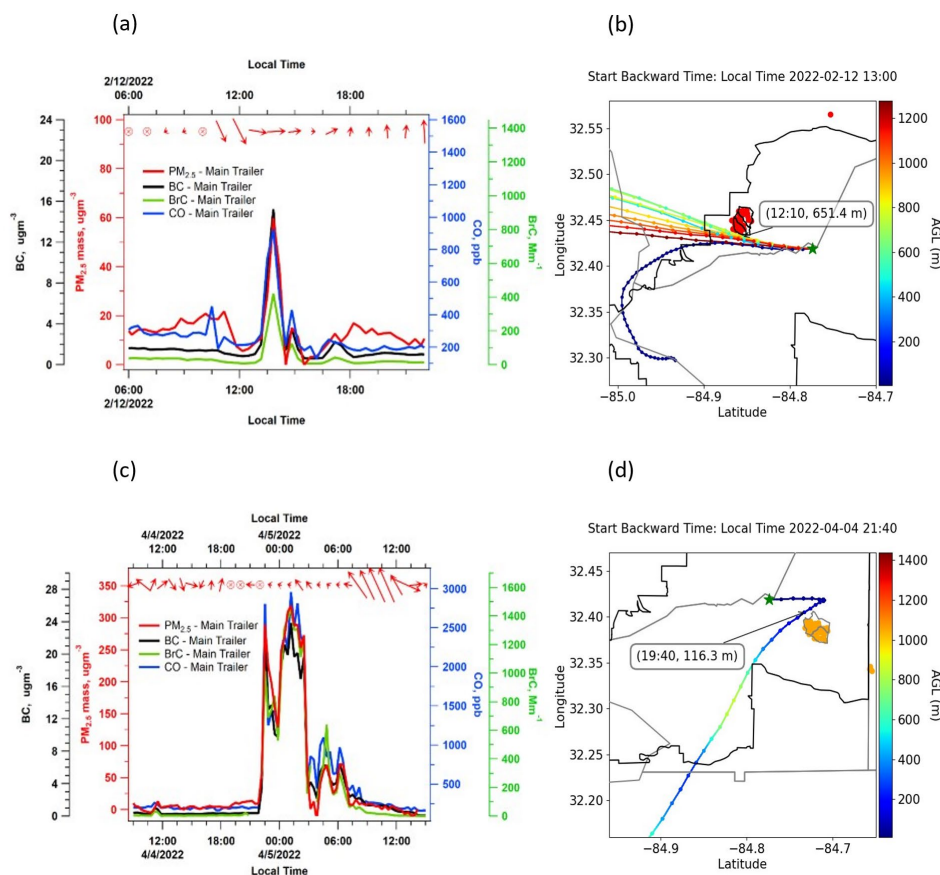
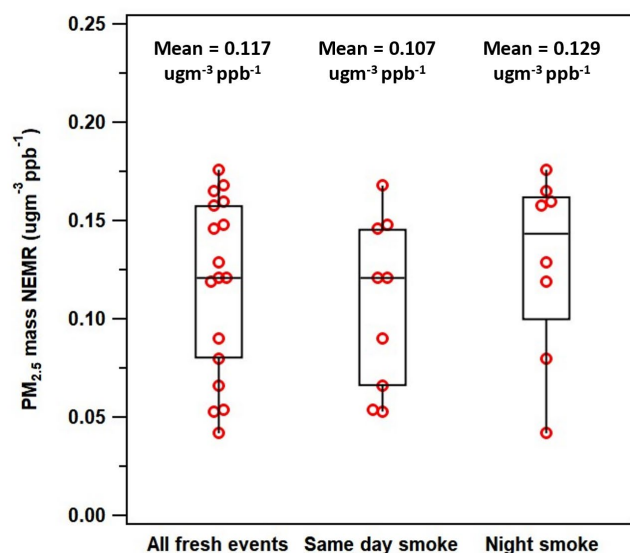


Figure S11. Two case studies with different dispersion conditions and PBL height. (a, b) Time series of species measured on main trailer. Time resolution is 20 minutes for CO, $\text{PM}_{2.5}$ mass, BC, and BrC. The wind vectors depict hourly data sourced from RAWS, with the direction of the arrow indicating wind direction and the length of the arrow representing wind speed. (b, d) HYSPLIT back trajectories starting on February 12, 2022 at 13:00 and April 4, 2022 at 21:40. The colors of the scatter are the height above ground level. Green star marks the location of the main trailer. Date and time of the backward trajectory is indicated on top of each map. Time and height at which the lowest trajectory crosses the trailer is shown in the box inside each map. Red dots are fires detected on FIRMS the same day of the backward trajectory (satellite overpass happened on February 12, 2022 at 13:54, 14:01, and on April 4, 2022 at 12:09, 14:49, and 15:36).

163



164

165 **Figure S12.** Box plot of PM_{2.5} mass NEMRs relative to CO (i.e., $\Delta\text{PM}_{2.5}\text{ mass}/\Delta\text{CO}$) of i) all fresh smoke
 166 events in this study, ii) fresh smoke from fires starting on the same day of the measurement, iii) fresh
 167 smoke from fires starting the day before measurement. The horizontal line inside the box represents the
 168 median of the data. The top line of the box represents the third quartile (Q3), and the bottom line
 169 represents the first quartile (Q1). There is no statistical difference between the two groups (two-tailed p
 170 value is 0.355).

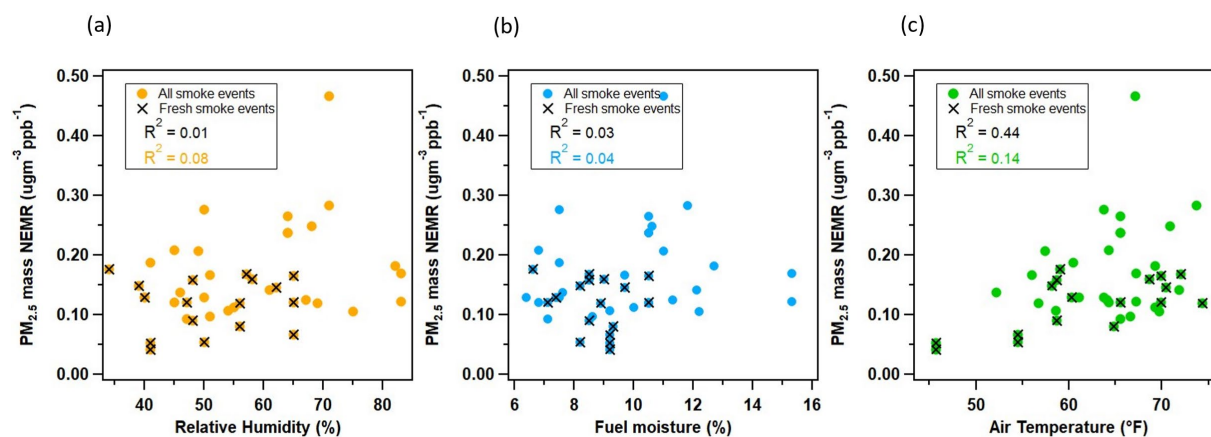
171

172

173

174

175



177

178 **Figure S13.** Variability of $PM_{2.5}$ mass NEMRs as a function of (a) relative humidity, (b) fuel moisture,
 179 and (c) air temperature. Meteorological data are from Fort Moore RAWS site (Figure 1a). The Pearson's
 180 correlation coefficients are shown in each plot for all smoke events (colored) and for fresh smoke plumes
 181 (≤ 1 hr old).

182

183 **Table S1.** Fire Information. Available as a separate excel file in the supplementary material.

184

185

186

187

Table S2. Monthly average backgrounds of PM_{2.5} mass, BC, and CO concentrations excluding peaks and the data 24 hours after each peak at each trailer during 2021 and 2022 field studies.

Month/Year	PM _{2.5} ug/m ³	CO ppb	BC ug/m ³
March 2021	4.67 ± 4.04 ^a	194.0 ± 41.1 ^a	0.32 ± 0.28 ^a
April 2021	3.74 ± 2.45 ^a	203.3 ± 31.0 ^a	0.35 ± 0.19 ^a
May 2021	2.78 ± 2.61 ^b	172.2 ± 23.5 ^b	0.22 ± 0.18 ^b
February 2022	3.12 ± 4.59 ^c	182.2 ± 32.3 ^c	0.38 ± 0.30 ^c
March 2022	2.55 ± 4.70 ^c	198.0 ± 26.9 ^c	0.21 ± 0.16 ^c
	5.02 ± 2.41 ^d	196.7 ± 37.0 ^d	0.19 ± 0.15 ^d
	4.80 ± 2.86 ^e	-	0.31 ± 0.26 ^e
	6.22 ± 2.02 ^f	-	-
	5.47 ± 2.47 ^g	-	-
April 2022	2.91 ± 4.20 ^c	177.7 ± 20.1 ^c	0.23 ± 0.20 ^c
	6.11 ± 3.58 ^d	191.8 ± 28.8 ^d	0.57 ± 0.31 ^d
	6.59 ± 2.79 ^e	-	0.23 ± 0.17 ^e
	6.30 ± 3.94 ^g	-	-
May 2022	2.48 ± 2.91 ^c	168.5 ± 22.6 ^c	0.14 ± 0.07 ^c
	6.27 ± 2.75 ^d	152.3 ± 34.7 ^d	0.26 ± 0.17 ^d
	6.80 ± 3.20 ^e	-	0.18 ± 0.08 ^e
	6.36 ± 3.31 ^f	150.8 ± 23.5 ^f	-
	6.10 ± 2.44 ^g	-	-
^a : trailer was located in the northwest corner of the Fort.			
^b : trailer was relocated to the central area of the Fort.			
^c : average calculated from measurements on the main trailer.			
^d : average calculated from measurements on trailer 1293.			
^e : average calculated from measurements on trailer 1292.			
^f : average calculated from measurements on trailer 1291.			
^g : average calculated from measurements on trailer 1290.			

192 **Table S3.** Monthly average backgrounds of PM_{2.5} mass concentrations (ug m⁻³) excluding peaks and the
 193 data 24 hours after each peak at EPD sites.

	Month/Year	Columbus Airport	Phenix City South Girard (PCSG) School
Mean	2021	8.99 ± 7.16	9.59 ± 7.90
	2022	10.33 ± 8.70	10.67 ± 9.40
Background	March 2021	9.10 ± 4.90	7.55 ± 5.21
	April 2021	6.44 ± 3.43	6.77 ± 2.92
	May 2021	6.40 ± 3.57	7.75 ± 3.75
	February 2022	-	8.01 ± 5.20
	March 2022	6.41 ± 3.75	6.22 ± 6.21
	April 2022	7.40 ± 3.50	8.03 ± 5.03
	May 2022	7.29 ± 2.76	6.72 ± 3.85

194

195

196 **Table S4.** Observed smoke peaks during the 2021 burning season in Fort Moore, GA, with their
 197 corresponding maximum values of 20 and 60 minutes averaged PM_{2.5} mass and CO concentrations.

Date	PM _{2.5} - 20 minute max ug m ⁻³	PM _{2.5} - 60 minute max ug m ⁻³	CO – 20 minute max ppb	CO – 60 minute max ppb
3/23/2021	74.8	54.7	638.4	509.3
3/30/2021	35.6	34.1	-	-
4/06/2021	74.9	66.9	772.7	707.6
4/07/2021	182.0	131.8	1184.6	964.3
4/08/2021	46.8	43.9	507.1	505.9
4/13/2021	39.0	37.1	-	-
4/14/2021	44.9	28.8	377.2	275.8
4/20/2021	69.9	50.7	1072.6	690.9
4/21/2021 (2 peaks)	118.5 2129.2 ^a	65.4 1408.2 ^a	1159.0 6260.4	925.4 6142.5
4/30/2021	46.8	39.9	551.5	500.7

^a: Filter was clogged due to a nearby fire and direct hit of smoke.
 In some cases CO data was not available and left as blank values (-) due to technical issue
 with the data acquisition system.

198

199

200 **Table S5.** Observed smoke peaks during the 2022 burning season in Fort Moore, GA, at the Main Trailer,
 201 with their corresponding maximum values of 20 and 60 minutes averaged PM_{2.5} mass and CO
 202 concentrations.

Date	PM _{2.5} – 20 minute max ug m ⁻³	PM _{2.5} – 60 minute max ug m ⁻³	CO – 20 minute max ppb	CO – 60 minute max ppb
2/11/2022	62.8	52.5	1336.6	972.0
2/12/2022	60.0	33.0	926.4	650.5
2/13/2022 (2peaks)	50.0 41.4	43.9 36.4	1041.4 1482.7	999.5 1069.7
2/26/2022	274.8	204.7	1344.2	1220.3
2/27/2022	46.6	31.2	456.4	360.7
3/01/2022	122.8	105.6	966.4	747.7
3/02/2022	118.3	89.7	1046.5	762.1
3/04/2022 (2 peaks)	38.4 100.4	28.8 79.9	411.8 947.1	352.2 715.0
3/05/2022	37.2	28.0	399.0	319.1
3/07/2022 (2 peaks)	64.4 45.2	57.3 35.9	583.9 429.7	503.8 396.6
3/14/2022	236.0	185.6	1362.9	1312.9
3/25/2022	52.2	45.6	596.6	454.8
3/29/2022	141.0	100.5	1145.0	855.6

4/04/2022	319.2	298.9	2960.1	2765.3
4/25/2022	60.7	50.7	394.7	323.5
5/09/2022	52.3	42.0	358.9	349.0

203

204

205 **Table S6.** Observed smoke peaks during the 2022 burning season in Fort Moore, GA, at Trailer 1293,
 206 with their corresponding maximum values of 20 and 60 minutes averaged PM_{2.5} mass and CO
 207 concentrations.

Date	PM _{2.5} – 20 minute max ug m ⁻³	PM _{2.5} – 60 minute max ug m ⁻³	CO – 20 minute max ppb	CO – 60 minute max ppb
3/21/2022	104.6	87.2	715.5	644.4
3/25/2022	52.9	33.7	455.3	344.0
3/26/2022	841.4	513.0	6044.5	3554.7
3/27/2022	170.8	141.2	1091.8	966.1
3/28/2022	80.7	42.5	875.1	692.4
3/29/2022	128.2	64.3	1574.4	887.9
4/05/2022	35.59	32.6	286.0	269.6
4/21/2022	39.8	32.1	228.5	214.2
4/23/2022 (2 peaks)	73.2 317.7	51.2 246.5	515.1 2104.9	348.4 1678.8
4/24/2022	133.1	123.9	662.1	611.1
4/26/2022	58.9	53.0	415.1	383.6
5/09/2022	40.2	34.7	311.4	288.7
5/10/2022	65.2	43.5	650.9	562.1
5/11/2022	147.6	104.2	826.4	711.9

5/12/2022 ^a	511.9	311.0	5108.2	2926.9
	506.2	444.5	4903.3	4381.4

^a: Levels stayed high for 6 hours and had two maxima.

208

209

210 **Table S7.** Observed smoke peaks during 2022 burning season in Fort Moore, GA, at Trailer 1292, with
 211 their corresponding maximum values of 20 and 60 minutes averaged PM_{2.5} mass concentrations.

Date	PM _{2.5} – 20 minute max ug m ⁻³	PM _{2.5} - hourly max ug m ⁻³
3/21/2022	63.4	60.6
3/22/2022	38.0	27.7
3/26/2022	52.5	49.0
3/27/2022 (2 peaks)	126.8 119.2	94.5 97.4
3/28/2022	117.4	108.9
3/29/2022	165.2	142.1
3/30/2022	37.4	34.4
4/11/2022	44.9	28.1
4/25/2022	64.4	45.2
4/29/2022	55.7	37.7
5/9/2022	52.8	42.3
5/10/2022	35.8	29.0

212

213

Table S8. Observed smoke peaks during the 2022 burning season in Fort Moore, GA, at Trailer 1291, with their corresponding maximum values of 20 and 60 minutes averaged PM_{2.5} mass and CO concentrations.

Date	PM _{2.5} - 20 minute max ug m ⁻³	PM _{2.5} - hourly max ug m ⁻³	CO -20 minute max ppb	CO - hourly max ppb
3/21/2022	51.2	34.6	-	-
3/27/2022	119.9	109.4	-	-
3/28/2022	159.4	118.4	-	-
3/29/2022	101.4	69.0	-	-
5/09/2022	69.2	56.5	427.8	356.2

In some cases CO data was not available and left as blank values (-) due to technical issue with the instrument or data acquisition system.

Table S9. Satellite overpasses (local time) during the three smoke episodes shown in Figure 5.

Hotspot	Time of Satellite overpass	Satellite
a, b	4/05/2021 11:52	Modis/Terra
a, b	4/05/2021 14:24	VIRS375m/Suomi NPP
a, b, c	4/05/2021 15:07	Modis/Aqua
a, b, c	4/05/2021 15:12	VIRS375/NOAA-20
d, e, f	4/06/2021 12:35	Modis/Terra
d, e, f	4/06/2021 14:00	VIRS375m/Suomi NPP
d, e	4/06/2021 14:12	Modis/Aqua
d, e, f	4/06/2021 14:54	VIRS375/NOAA-20
g	4/07/2021 11:39	Modis/Terra
g	4/07/2021 14:36	VIRS375/NOAA-20
g	4/07/2021 14:55	Modis/Aqua
g	4/07/2021 15:24	VIRS375m/Suomi NPP

232 **Table S10.** Age estimates of identified smoke events using average wind vector and HYSPLIT model.

Date	Site	Source Identification Method	Age – using average wind vector	Age – HYSPLIT back trajectory
3/23/2021	Main Trailer	Methods agree	1 hr 48 min	40 min
3/30/2021	Main Trailer	HYSPLIT	-	2 hr 30 min
4/06/2021	Main Trailer	Methods agree	1 hr 15 min	2 hr 10 min
4/07/2021	Main Trailer	Methods agree	14 min	10 min
4/08/2021	Main Trailer	Methods agree	162 min	40 min
4/13/2021	Main Trailer	Methods agree	-	20 min
4/14/2021	Main Trailer	Methods agree	44 min	20 min
4/20/2021	Main Trailer	Methods agree	Few minutes	10 min
4/21/2021 (2 peaks)	Main Trailer	Methods disagree	5 hr 30 min	3 hr 10 min
4/30/2021	Main Trailer	Methods agree	Few minutes	10 min
	Main Trailer	Unidentified	-	-
2/11/2022	Main Trailer	Methods agree	8 min	10 min
2/12/2022	Main Trailer	Methods agree	60 min	50 min
2/13/2022 (2 peaks)	Main Trailer	Methods agree	26 min	20 min
	Main Trailer	Methods agree	30 min	20 min
2/26/2022	Main Trailer	Methods disagree	2 hr 10 min	1 hr 50 min
2/27/2022	Main Trailer	Methods disagree	Residual/high background	Residual/high background
3/01/2022	Main Trailer	Methods disagree	1 hr 32 min	4 hr 30 min

3/02/2022	Main Trailer	Methods agree	60 min	40 min
3/04/2022 (2 peaks)	Main Trailer	HYSPLIT	-	2 hr 40 min
	Main Trailer	HYSPLIT	-	40 min
3/05/2022	Main Trailer	Unidentified	-	-
3/07/2022 (2 peaks)	Main Trailer	Wind vector	224 min	-
	Main Trailer	HYSPLIT	-	10 min
3/14/2022	Main Trailer	HYSPLIT	-	20 min
3/25/2022	Main Trailer	Methods agree	Few minutes	10 min
3/29/2022	Main Trailer	Methods agree	Few minutes	10 min
4/04/2022	Main Trailer	Methods agree	2 hr 48 min	2hr 10min
4/25/2022	Main Trailer	Methods agree	2 hr 49 min	1hr 30 min
5/09/2022	Main Trailer	Methods agree	5 hr 30 min	2 hr 30 min
3/21/2022	T1293	Methods agree	1 hr 29 min	20 min
3/25/2022	T1293	Methods agree	45 min	30 min
3/26/2022	T1293	Methods agree	Few minutes	10 min
3/27/2022	T1293	Methods agree	Few minutes	10 min
3/28/2022	T1293	Methods agree	-	60 min
3/29/2022	T1293	Methods disagree	-	3 hr 30 min
4/05/2022	T1293	HYSPLIT	-	6 hr
4/21/2022	T1293	Wind vector	78 min	-

4/23/2022	T1293	Methods agree	28 min	10 min
(2 peaks)		Methods agree	48 min	10 min
4/24/2022	T1293	Methods agree	63 min	40 min
4/26/2022	T1293	Wind vector	1 hr 46 min	-
5/09/2022	T1293	Methods agree	8 hr	3 hr 30 min
5/10/2022	T1293	Methods agree	7 hr 54 min	2 hr 40 min
5/11/2022	T1293	Methods agree	Few minutes	10 min
5/12/2022	T1293	Methods agree	Few minutes	10 min
3/21/2022	T1292	Methods agree	-	60 min
3/22/2022	T1292	HYSPLIT	-	40 min
3/26/2022	T1292	Methods agree	45 min	30 min
3/27/2022	T1292	Methods agree	36 min	20 min
(2 peaks)	T1292	Methods agree	1 hr 27 min	20 min
3/28/2022	T1292	Methods agree	10 min	20 min
3/29/2022	T1292	Methods disagree	59 min	20 min
3/30/2022	T1292	Methods agree	1 hr 18 min	20 min
4/11/2022	T1292	Wind vector	1 hr 19 min	-
4/25/2022	T1292	Methods agree	3 hr 37 min	1 hr 50 min
4/29/2022	T1292	Unidentified	-	-
5/09/2022	T1292	Methods agree	4hr 56 min	2 hr 40 min

5/10/2022	T1292	Wind vector	1hr 25 min	-
3/21/2022	T1291	Methods agree	3 hr 42 min	1 hr 20 min
3/27/2022	T1291	Methods agree	63 min	30 min
3/28/2022	T1291	Methods agree	54 min	2 hr 10 min
3/29/2022	T1291	Methods disagree	1 hr 18 min	40 min
5/09/2022	T1291	Methods agree	4 hr 26 min	1 hr 30 min

233

234

235

236 **Table S11.** PM_{2.5} mass NEMRs ($\mu\text{g m}^{-3}$ ppb⁻¹) from other studies used in the comparison conducted with
 237 our findings.

Study	PM _{2.5} mass NEMR ($\mu\text{g m}^{-3}$ ppb ⁻¹)	Platform used	Type	Estimated Age as reported
(Alves et al., 2010) ^a	0.121	Ground	Prescribed fires/ shrub-dominant forests with some pine trees in Portugal	Fresh
(Desservettaz et al., 2017) ^{a,b}	0.069	Ground	Prescribed fires/ tropical savanna forests in Australia	1 min
	0.037			10 min
	0.080			10 min
	0.103			20 min
(Korontzi et al., 2003)	0.084	Ground	Prescribed fires/ grassland ecosystems in southern Africa	Fresh
	0.075			
	0.077			
	0.069			
	0.097			
	0.114			
	0.108			
	0.102			
	0.091			
	0.106			
(Balachandran et al., 2013) ^a	0.151	Ground	Prescribed fires/ grass and longleaf pine ecosystems in Georgia	30-105 min
	0.186			
(Sinha et al., 2003) ^c	0.200	Airborne	Prescribed fires/ savanna forests in southern Africa	Few min
(Travis et al., 2023) ^f	0.188	Airborne	Prescribed fires/ slash, piles, grassland, shrubland in eastern USA	Fresh
	0.196			
	0.304			
	0.433			
(May et al., 2014) ^{a,b}	0.115	Airborne	Prescribed fires/ chaparral and montane ecosystems in CA; coastal plain ecosystem in SC	Fresh
	0.043			
	0.055			
(May et al., 2015) ^{b,e}	0.031	Airborne	Prescribed fires/ South Carolina	Fresh
(Liu et al., 2017) ^{a,f}	0.045	Airborne	Wildfires/ western US	< 20 min 1 h
	0.427			
	0.307			
(Palm et al., 2020) ^b	0.298	Airborne	Wildfires/ western US	20 min – 2 h 1 h
	0.250			

(Collier et al., 2016) ^b	0.210	Airborne	Wildfires/ northwest US	1 h
	0.270			1 h
	0.240			1 h
	0.240			1 h
	0.320			1 h
	0.390			1 h
	0.330			1 h
	0.310			1 h
	0.260			1 h
	0.170			2 h
	0.290			4 h
	0.370			3 h
	0.290			3 h
	0.250			3 h
(Gkatzelis et al., 2024) ^{a,g}	0.421	Airborne	Western US wildfires. Understory; Savanna; Shrubland; Grassland; Forest land	21 min
	0.194			10 min
	0.142			29 min
	0.228			43 min
	0.159			25 min
	0.331			15 min
	0.524			102 min
	0.398			65 min
	0.391			104 min
	0.178			91 min
	0.204			25 min
	0.463			153 min
	0.244			27 min
	0.039			20 min
	0.462	Airborne	Eastern US prescribed fire of forest land	10 min

238 ^a: $\Delta\text{PM}_{2.5}/\Delta\text{CO}$ reported in g g^{-1} was converted to $\mu\text{g m}^{-3} \text{ppb}^{-1}$ through division by 24.45/molar mass of
239 CO (28.01 g mol^{-1})

240 ^b: values correspond to $\Delta\text{OA}/\Delta\text{CO}$

241 ^c: values correspond to $\Delta\text{PM}_4/\Delta\text{CO}$

242 ^d: values correspond to $(\text{OA}/\text{CO}_2 \text{ in } \text{g g}^{-1})/(\text{CO}/\text{CO}_2 \text{ in } \text{g g}^{-1})$. Molar ratio of CO/CO₂ (mol/mol) was
243 converted to mass ratio (g g^{-1}) by multiplying by molar mass of CO (28.01 g mol^{-1})/molar mass of CO₂
244 (44.01 g mol^{-1})

245 ^e: values were inferred from the box plots in Figures 2 and 3 for the freshest smoke measured

246 ^f: values correspond to $\Delta\text{PM}_1/\Delta\text{CO}$

247 ^g: values correspond to $(\text{OA} + \text{particulate nitrate} + \text{particulate ammonium} + \text{BC})/\text{CO}$

248

249

References

- Alves, C. A., Gonçalves, C., Pio, C. A., Mirante, F., Caseiro, A., Tarelho, L., Freitas, M. C., and Viegas, D. X.: Smoke emissions from biomass burning in a Mediterranean shrubland, *Atmos. Environ.*, 44, 3024–3033, <https://doi.org/10.1016/j.atmosenv.2010.05.010>, 2010.
- Balachandran, S., Pachon, J. E., Lee, S., Oakes, M. M., Rastogi, N., Shi, W., Tagaris, E., Yan, B., Davis, A., Zhang, X., Weber, R. J., Mulholland, J. A., Bergin, M. H., Zheng, M., and Russell, A. G.: Particulate and gas sampling of prescribed fires in South Georgia, USA, *Atmos. Environ.*, 81, 125–135, <https://doi.org/10.1016/j.atmosenv.2013.08.014>, 2013.
- Collier, S., Zhou, S., Onasch, T. B., Jaffe, D. A., Kleinman, L., Sedlacek, A. J., Briggs, N. L., Hee, J., Fortner, E., Shilling, J. E., Worsnop, D., Yokelson, R. J., Parworth, C., Ge, X., Xu, J., Butterfield, Z., Chand, D., Dubey, M. K., Pekour, M. S., Springston, S., and Zhang, Q.: Regional Influence of Aerosol Emissions from Wildfires Driven by Combustion Efficiency: Insights from the BBOP Campaign, *Environ. Sci. Technol.*, 50, 8613–8622, <https://doi.org/10.1021/acs.est.6b01617>, 2016.
- Desservettaz, M., Paton-Walsh, C., Griffith, D. W. T., Kettlewell, G., Keywood, M. D., Vanderschoot, M. V., Ward, J., Mallet, M. D., Milic, A., Miljevic, B., Ristovski, Z. D., Howard, D., Edwards, G. C., and Atkinson, B.: Emission factors of trace gases and particles from tropical savanna fires in Australia, *J. Geophys. Res. Atmos.*, 122, 6059–6074, <https://doi.org/10.1002/2016JD025925>, 2017.
- Gkatzelis, G. I., Coggon, M. M., Stockwell, C. E., Hornbrook, R. S., Allen, H., Apel, E. C., Bela, M. M., Blake, D. R., Bourgeois, I., Brown, S. S., Campuzano-Jost, P., St. Clair, J. M., Crawford, J. H., Crounse, J. D., Day, D. A., DiGangi, J. P., Diskin, G. S., Fried, A., Gilman, J. B., Guo, H., Hair, J. W., Halliday, H. S., Hanisco, T. F., Hannun, R., Hills, A., Huey, L. G., Jimenez, J. L., Katich, J. M., Lamplugh, A., Lee, Y. R., Liao, J., Lindaas, J., McKeen, S. A., Mikoviny, T., Nault, B. A., Neuman, J. A., Nowak, J. B., Pagonis, D., Peischl, J., Perring, A. E., Piel, F., Rickly, P. S., Robinson, M. A., Rollins, A. W., Ryerson, T. B., Schueneman, M. K., Schwantes, R. H., Schwarz, J. P., Sekimoto, K., Selimovic, V., Shingler, T., Tanner, D. J., Tomsche, L., Vasquez, K. T., Veres, P. R., Washenfelder, R., Weibring, P., Wennberg, P. O., Wisthaler, A., Wolfe, G. M., Womack, C. C., Xu, L., Ball, K., Yokelson, R. J., and Warneke, C.: Parameterizations of US wildfire and prescribed fire emission ratios and emission factors based on FIREX-AQ aircraft measurements, *Atmos. Chem. Phys.*, 24, 929–956, <https://doi.org/10.5194/acp-24-929-2024>, 2024.
- Korontzi, S., Ward, D. E., Susott, R. A., Yokelson, R. J., Justice, C. O., Hobbs, P. V., Smithwick, E. A. H., and Hao, W. M.: Seasonal variation and ecosystem dependence of emission factors for selected trace gases and PM 2.5 for southern African savanna fires, *J. Geophys. Res. Atmos.*, 108,

282 <https://doi.org/10.1029/2003JD003730>, 2003.

283 Liu, X., Huey, L. G., Yokelson, R. J., Selimovic, V., Simpson, I. J., Müller, M., Jimenez, J. L.,
 284 Campuzano-Jost, P., Beyersdorf, A. J., Blake, D. R., Butterfield, Z., Choi, Y., Crounse, J. D., Day, D. A.,
 285 Diskin, G. S., Dubey, M. K., Fortner, E., Hanisco, T. F., Hu, W., King, L. E., Kleinman, L., Meinardi, S.,
 286 Mikoviny, T., Onasch, T. B., Palm, B. B., Peischl, J., Pollack, I. B., Ryerson, T. B., Sachse, G. W.,
 287 Sedlacek, A. J., Shilling, J. E., Springston, S., St. Clair, J. M., Tanner, D. J., Teng, A. P., Wennberg, P.
 288 O., Wisthaler, A., and Wolfe, G. M.: Airborne measurements of western U.S. wildfire emissions:
 289 Comparison with prescribed burning and air quality implications, *J. Geophys. Res. Atmos.*, 122, 6108–
 290 6129, <https://doi.org/10.1002/2016JD026315>, 2017.

291 May, A. A., McMeeking, G. R., Lee, T., Taylor, J. W., Craven, J. S., Burling, I., Sullivan, A. P., Akagi,
 292 S., Collett, J. L., Flynn, M., Coe, H., Urbanski, S. P., Seinfeld, J. H., Yokelson, R. J., and Kreidenweis, S.
 293 M.: Aerosol emissions from prescribed fires in the United States: A synthesis of laboratory and aircraft
 294 measurements, *J. Geophys. Res. Atmos.*, 119, 11,826–11,849, <https://doi.org/10.1002/2014JD021848>,
 295 2014.

296 May, A. A., Lee, T., McMeeking, G. R., Akagi, S., Sullivan, A. P., Urbanski, S., Yokelson, R. J., and
 297 Kreidenweis, S. M.: Observations and analysis of organic aerosol evolution in some prescribed fire smoke
 298 plumes, *Atmos. Chem. Phys.*, 15, 6323–6335, <https://doi.org/10.5194/acp-15-6323-2015>, 2015.

299 National Centers for Environmental Prediction, National Weather Service, NOAA, U. S. D. of C.: NCEP
 300 ADP Global Surface Observational Weather Data, October 1999 - continuing, 2004a.

301 National Centers for Environmental Prediction, National Weather Service, NOAA, U. S. D. of C.: NCEP
 302 ADP Global Upper Air Observational Weather Data, October 1999 - continuing, 2004b.

303 Palm, B. B., Peng, Q., Fredrickson, C. D., Lee, B. H., Garofalo, L. A., Pothier, M. A., Kreidenweis, S.
 304 M., Farmer, D. K., Pokhrel, R. P., Shen, Y., Murphy, S. M., Permar, W., Hu, L., Campos, T. L., Hall, S.
 305 R., Ullmann, K., Zhang, X., Flocke, F., Fischer, E. V., and Thornton, J. A.: Quantification of organic
 306 aerosol and brown carbon evolution in fresh wildfire plumes, *Proc. Natl. Acad. Sci.*, 117, 29469–29477,
 307 <https://doi.org/10.1073/pnas.2012218117>, 2020.

308 Sinha, P., Hobbs, P. V., Yokelson, R. J., Bertschi, I. T., Blake, D. R., Simpson, I. J., Gao, S., Kirchstetter,
 309 T. W., and Novakov, T.: Emissions of trace gases and particles from savanna fires in southern Africa, *J.*
 310 *Geophys. Res. Atmos.*, 108, <https://doi.org/10.1029/2002JD002325>, 2003.

311 Travis, K. R., Crawford, J. H., Soja, A. J., Gargulinski, E. M., Moore, R. H., Wiggins, E. B., Diskin, G.
 312 S., DiGangi, J. P., Nowak, J. B., Halliday, H., Yokelson, R. J., McCarty, J. L., Simpson, I. J., Blake, D.

313 R., Meinardi, S., Hornbrook, R. S., Apel, E. C., Hills, A. J., Warneke, C., Coggon, M. M., Rollins, A. W.,
314 Gilman, J. B., Womack, C. C., Robinson, M. A., Katich, J. M., Peischl, J., Gkatzelis, G. I., Bourgeois, I.,
315 Rickly, P. S., Lamplugh, A., Dibb, J. E., Jimenez, J. L., Campuzano-Jost, P., Day, D. A., Guo, H.,
316 Pagonis, D., Wennberg, P. O., Crounse, J. D., Xu, L., Hanisco, T. F., Wolfe, G. M., Liao, J., St. Clair, J.
317 M., Nault, B. A., Fried, A., and Perring, A. E.: Emission Factors for Crop Residue and Prescribed Fires in
318 the Eastern US During FIREX-AQ, *J. Geophys. Res. Atmos.*, 128,
319 <https://doi.org/10.1029/2023JD039309>, 2023.

320